

PACS numbers: 43.35.Ns, 68.60.Bs

INFLUENCE OF THERMAL ANNEALING ON STRUCTURAL AND ELECTRICAL PROPERTIES OF NICKEL OXIDE THIN FILMS

**A. Mallikarjuna Reddy¹, Ch. Seshendra Reddy¹, A. Sivasankar Reddy²,
P. Sreedhara Reddy¹**

¹ Department of Physics
Sri Venkateswara University, Tirupati-517502, India
E-mail: malliphysics@gmail.com

² Division of Advanced Material Science and Engineering,
Kongju National University, Kongju City 182, Republic of Korea

Nickel oxide (NiO) is a potential p-type transparent conducting oxide material with suitable electrical properties. Nickel oxide thin films were deposited by dc reactive magnetron sputtering technique on unheated glass substrates, and subsequently annealed at 773 K in two different annealing processes. X-ray diffractometer studies revealed that the films exhibited (200) preferred orientation. Scanning electron microscopy and energy dispersive spectroscopy were used to study the effect of annealing temperature on surface morphology and composition of the films. The uniform grains were distributed throughout the substrate after annealed at 773 K. Electrical properties were studied by Hall effect measurements. The low electrical resistivity of 36.9 Ω cm was observed after annealing.

Keywords: SPUTTERING, STRUCTURAL PROPERTIES, ELECTRICAL PROPERTIES, ANNEALING TEMPERATURE.

(Received 04 February 2011, in final form 01 May 2011)

1. INTRODUCTION

Transparent conducting oxide films such as zinc oxide, tin oxide, indium tin oxide are in practical use for transparent electrodes and window coatings [1-4]. All these films are n-type semiconductors. But transparent conducting thin film coatings of p-type semiconductors are required in applications such as transparent electrodes for optoelectronic devices, which make use of hole injection. Nickel oxide (NiO) is a model p-type semiconductor with band gap energy in the range 3.6-4.0 eV and it is an attractive material for transparent conducting oxide (TCO) applications [5]. Being an electrochromic material, NiO films have also found potential applications in energy efficient smart windows with controllable throughput of radiant energy, mirrors with variable reflectance and high contrast non-emissive information displays. It is well known for its chemical stability as well as for its excellent optical and electrical properties. It is evident that the improvement of the material properties can be reached by the optimization of the preparation conditions. Various methods were used to prepare nickel oxide films such as sputtering [6, 7], electron beam evaporation [8, 9], plasma-enhanced chemical vapour deposition [10], chemical bath deposition [11] and sol-gel [12]. Among these methods, dc reactive sputtering has been most widely useful technique having high deposition rates, uniformity over large areas of the substrates and easy

control over the composition of the deposited films. The properties of the deposited films depend on the deposition parameters such as substrate temperature, oxygen partial pressure, sputtering power, sputtering pressure, substrate bias voltage and annealing temperature. In the present study, NiO thin films were deposited on unheated substrates by using dc reactive magnetron sputtering technique and studied the effect of annealing temperature on the properties of the films. The as deposited films were annealed at 773 K in two different annealing processes. In the first process, the annealing temperature increased continuously up to 773 K, and then the films were annealed 2 h 30 min at this temperature (set 1). In second process, the films were annealed 30 min at every 100 K up to 773 K (set 2).

2. EXPERIMENTAL DETAILS

NiO thin films were grown on Corning 7059 glass substrates by using the dc reactive magnetron sputtering from a homemade circular planar magnetron sputtering system. The sputtering system is capable of creating an ultimate vacuum of 5×10^{-4} Pa. The sputter chamber was pumped with diffusion pump and rotary pump combination. The pressure in the sputter chamber was measured using digital Pirani and Penning gauge combination. A circular planar magnetron of 100 mm diameter was used as the magnetron cathode. The magnetron target assembly was mounted on the top of the sputter chamber such that the sputtering could be done by sputter down configuration. A continuously variable dc power supply of 1000 V and 1 A was used as a power source for sputtering. A 100 mm diameter and 3 mm thick pure nickel (99.98 %) was used as sputter target. Pure argon was used as sputter gas and oxygen as reactive gas. The flow rates of both argon and oxygen gases were controlled individually by Tylan mass flow controllers. Before deposition of each film, the target was sputtered in pure argon atmosphere for 10 min to remove oxide layer if any on the surface of the target. The sputtering conditions maintained during the growth of NiO films were given in Table 1.

Table 1 – Deposition parameters maintained during the deposition of NiO films by dc reactive magnetron sputtering

Sputtering target (Pure Nickel (99.98 %))	100 mm dia 3 mm thick
Target to substrate distance	70 mm
Substrate	Corning 7059 glass
Ultimate pressure	5×10^{-4} Pa
Oxygen partial pressure (p_{O_2})	6×10^{-2} Pa
Sputtering pressure (P_w)	4 Pa
Sputtering power (W)	150 W
Annealing temperature	773 K

The deposited films were characterized by studying crystallographic structure, micro-structural, and electrical properties. The crystallographic structure of the films was analyzed by X-ray diffractometer using CuK α radiation ($\lambda = 0.1546$ nm) of model 3033TT manufactured by Seifert. The microstructure of the films was studied by Carl Zeiss EVO MA 15 scanning electron microscope (SEM) for which an EDS is attached of model Inca Penta

FETx3 manufactured by Oxford Instruments was used for composition analysis. The electrical resistivity and Hall mobility were studied by employing the van der Pauw method [13].

The sheet resistance (ρ_s) of the films was calculated using the equation,

$$\rho_s = (\pi/\ln 2)f[(R_1 + R_2)/2], \quad (1)$$

where f is the van der Pauw correction factor, which depends on the position of electrical contacts on the film surface,

$$f = (1 - \ln 2/2)[(R_1 - R_2)/(R_1 + R_2)]^2. \quad (2)$$

The electrical resistivity (ρ) of the films was determined from the relation

$$\rho = \rho_s \cdot t, \quad (3)$$

where t is the film thickness. The Hall mobility (μ) of the films was calculated from the relation,

$$\mu = (\Delta R \cdot 10^8) B \rho_s, \quad (4)$$

where ΔR is the change of resistance with the applied magnetic field (B).

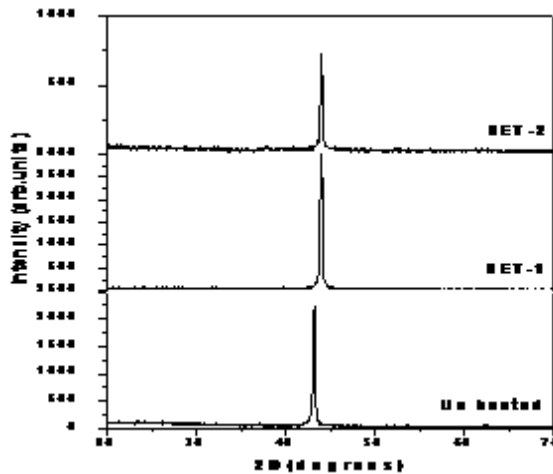
3. RESULTS AND DISCUSSION

3.1 Structural properties

Fig. 1 shows the XRD patterns of as deposited and annealed NiO films. From the XRD patterns, the films exhibited (200) preferred orientation and the 2θ values were shifted towards the higher degree after annealing. The improvement in crystallinity of the films was more favoured in set 1 samples as compared to set 2. This may be due to increase of average crystallite size with the increase of the annealing temperature which can be related to the interface merging processes induced by the thermal annealing. The interface reactions can be related to the existence of interface defects at the grain or crystallite boundaries. At the crystallite boundaries there are many Ni or O₂ defects (dangling bonds). These defects were amenable to the merging process, resulting in larger grains or crystallites. In addition, the merging process was also indicated by the increase in the intensities of the diffraction peaks with the annealing temperature. The films deposited on unheated substrates have low atomic mobility and tends to form preferred crystallite structure [14]. The increased intensity of the (200) peak with increasing the annealing temperature to 773 K may be due to an increase in the size of the grains. The lattice parameter of the films was also influenced by the annealing temperature. The present obtained lattice parameter of annealed films is lower than the standard bulk NiO. Where as the lattice parameter of the film deposited on unheated substrate is higher than the standard value.

The variation in the lattice parameter with annealing temperature was due to the stresses developed in the films. The stress (σ) developed in the films was calculated from the X-ray diffraction data employing the relation [15],

$$\sigma = -E(a - a_0)/2va_0, \quad (5)$$

**Fig. 1 – XRD Patterns of NiO thin films**

where E is the Young modulus of the NiO (200 GPa), a is the lattice parameter of the bulk material, a_0 is the measured lattice parameter and ν is the Poisson ratio (0.31). The stress developed in the films was obtained by the shift in the interplanar spacing hence change in the lattice parameter. The lattice parameter, grain size and stress of the NiO films in two types of annealing temperature were given in Table 2. The grain size (L) of the films was calculated for (200) peak by using Scherrer equation.

$$L = \frac{K\lambda}{\beta \cos \theta}, \quad (6)$$

where K is the correction factor, λ is the wavelength of the incident beam, β is the full width at half maximum corresponding to diffraction angle θ .

Table 2 – The lattice parameter, grain size and stress of the NiO films as a function of annealing temperature

Annealing temperature	Orientation	Lattice parameter (nm)	Grain size (nm)	Stress (GPa)
Unheated substrate	(200)	0.4191	28	1.1587
Set 1	(200)	0.4118	34	- 4.5436
Set 2	(200)	0.4115	31	- 4.7022

3.2 Surface morphology

The scanning electron microscopy images of NiO films were shown in Fig. 2 a, c, f. From the micrographs, smooth surface was observed in the films deposited on unheated substrates. The fine grains were appeared when the films were annealed in both annealing processes. From the EDS results, higher oxygen content was observed in unheated substrate deposited films.

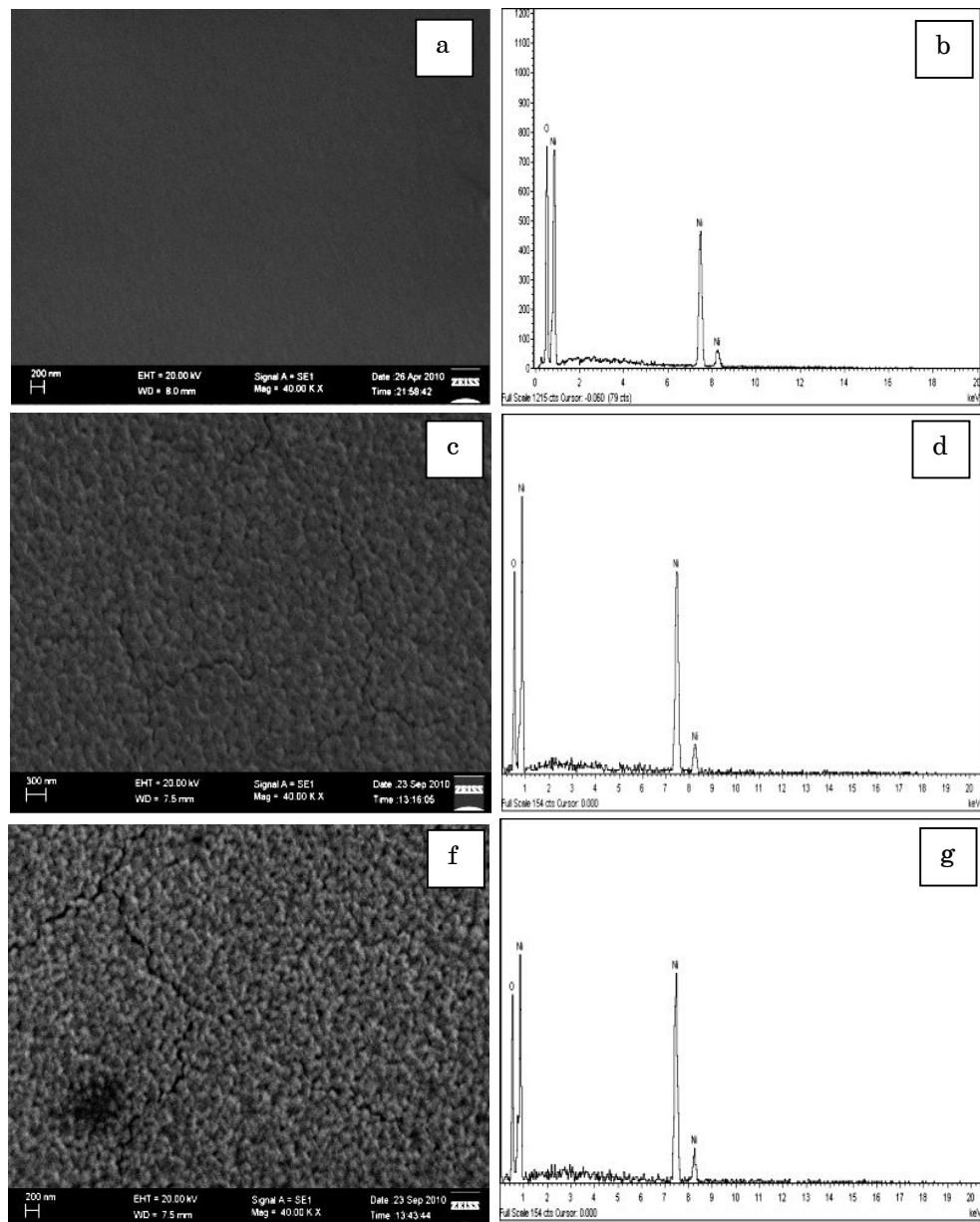


Fig. 2 – SEM images of NiO thin films on unheated substrate (a) Set1 (c) Set 2 (f) and EDS images of NiO thin films on unheated substrate (b) Set1 (d) Set2 (g)

After annealing (set 1 & 2), the stoichiometry of the films was improved. The compositional results were shown in Fig. 2 b, d, g and listed in Table 3.

Table 3 – The compositional analysis of dc reactive magnetron sputtered NiO thin films

Annealing temperature	Element	Weight %	Atomic %	Ni/O ratio
Unheated substrate	Ni K	37.05	31.65	0.46
	O K	62.95	68.35	
Set 1	Ni K	27.58	58.29	1.39
	O K	72.42	41.71	
Set 2	Ni K	27.11	57.71	1.36
	O K	72.89	42.29	

3.3 Electrical properties

The electrical resistivity of NiO thin films has a strong dependence on the microstructural defects existing in NiO crystallites, such as nickel vacancies and interstitial defects [16]. It is clear that electrical properties of NiO thin films were greatly affected by annealing temperature. The unheated substrate deposited films showed high electrical resistivity of $135.8 \Omega \text{ cm}$. The resistivity of the films annealed at 773 K in both type of annealing was low compared to unheated substrate deposited films. The detailed information on electrical properties was given in the Table 4.

Table 4 – The electrical properties of NiO thin films in both types of annealing

Sample information	Resistivity ($\Omega \text{ cm}$)	Carrier concentration (cm^{-3})	Mobility ($\text{cm}^2\text{V}^{-1}\text{s}^{-1}$)
Unheated substrate	135.8	2.6×10^{16}	1.8
Set 1	36.9	5.4×10^{16}	3.1
Set 2	39.4	5.3×10^{16}	3.0

4. CONCLUSIONS

Polycrystalline Nickel oxide thin films were successfully deposited by dc reactive magnetron sputtering at room temperature and annealed in two different processes. The as deposited and annealed films showed cubic structure. The set 1 films exhibited superior structural properties as compared to as deposited and set 2 films. After annealing, the stoichiometry of the films was progressively improved. The set 1 and set 2 films exhibited similar electrical properties and no considerable changes observed in the two different processes.

REFERENCES

1. K.G. Gopchandran, B. Joseph, J.T. Abraham, P. Koshy, V.K. Vaidyan, *Vacuum* **48**, 547 (1997).
2. P. Koshy, P.S. Mukherjee, K.G.K. Warrier, V.K. Vaidyan, *J. Mater. Sci. Lett.* **14**, 440 (1995).
3. J. Benny, K.G. Gopchandran, P.V. Thomas, P. Koshy, V.K. Vaidyan, *Mater. Chem. Phys.* **58**, 71 (1999).

4. K.L. Chopra, S. Major, D.K. Pandya, *Thin Solid Films* **102**, 1 (1983).
5. H. Sato, T. Minami, S. Takata, T. Yamada, *Thin Solid Films* **236**, 27 (1993).
6. S. Nishizawa, T Tsurumi, H Hyodo, Y Ishibashi, N Ohashi, M Ya-mane, O Fukunaga, *Thin Solid Films* **302**, 133 (1997).
7. G.H Yu, L.R Zen, F.W Zhu, C.L Chai, W.Y Lai, *J Appl. Phys.* **90**, 4039 (2001).
8. C.R. Otterman, A. Temmink, K. Bange, *Thin Solid Films* **193/194**, 409 (1990).
9. T. Seike, J. Nagai, *Sol. Energ. Mater.* **22**, 107 (1991).
10. W.C. Yeh, M. Matsumura *Jpn. J. Appl. Phys.* **36**, 6884 (1997).
11. X.H. Xia, J.P. Tu, J. Zhang, X.L. Wang, W.K. Zhang, H. Huang. *Sol. Energ. Mat. Sol. C.* **92**, 628 (2008).
12. L. Wang, Z. Zhang, Y. Cao, *J. Ceram. Soc. Jpn* **101**, 227 (1993).
13. L.J. van der Pauw, *Philips Res. Rep.* **13**, 1 (1958).
14. H.L. Chen, Y.M. Lu, W.S. Hwang, *Surf. Coat. Tech.* **198**, 138 (2005).
15. M. Ohring, *The material science of Thin Solid Films*, Academic Press (New York, 1992).
16. E. Antolini, *J. Mater. Sci.* **27**, 3335 (1992).